INSTITUTE FOR FUSION STUDIES

DOE/ET-53088-535 IFSR #535

Magnetic Surfaces in a Steady-State Tokamak

R. KINNEY, T. TAJIMA
Institute for Fusion Studies
The University of Texas at Austin
Austin, Texas 78712
and
H. IRIE
Department of Physics
Nihon University 1-8
Kanda Surugadai, Chiyoda-ku
Tokyo 101, Japan

February 1992

THE UNIVERSITY OF TEXAS

AUSTIN

Magnetic Surfaces in a Steady-State Tokamak

R. Kinney, T. Tajima
Institute for Fusion Studies
The University of Texas at Austin
Austin, Texas 78712
and
H. Irie
Department of Physics
Nihon University 1-8
Kanda Surugadai, Chiyoda-ku
Tokyo 101, Japan

Abstract

We study a toroidal plasma in a tokamak with externally given toroidal and poloidal magnetic fields as well as self-consistently interacting internal currents. The unperturbed magnetic surfaces are described by the well-known nonlinear "standard map." When the magnetic field is allowed to carry an internal current, the self-interaction of these currents disturbs the integrity of the magnetic surfaces. We carry out a computational study of the effects of the interacting internal current filaments, measuring the diffusion of field lines from the unperturbed surfaces, and find the self-interaction to be a significant effect which always serves to increase diffusion. Perfect surfaces are difficult to maintain even when magnetic islands do not overlap. Diffusion from the current interaction dominates when current fluctuations reach $\sim$ 10% of the applied field.

I. Introduction

The tokamak, as a toroidal plasma containment device, does exhibit evidence of possessing a natural current profile, just as in other devices, such as the reversed field pinch (RFP). This is in spite of the fact that, unlike some fusion devices, the tokamak cannot be said to undergo relaxation. Relaxed profiles for such experiments as RFP's can be obtained by assuming that the plasma undergoes a period of strong turbulence, during which the magnetic field memory is destroyed and energy is dissipated subject to the constraint that the global magnetic helicity remains constant [1]. Thus, a variational principle can predict the relaxed state of the plasma by minimizing the magnetic energy while helicity remains constant. There have also been variational treatments in which complete relaxation of the plasma is not assumed to take place, and the helicity density is conserved locally [2].

In a tokamak the physical justification for such a method is absent, because such strong turbulence does not occur during the device's normal operation, though such variational calculations have been carried out for the tokamak, and do lead to plausible profiles [3, 4, 5]. Taylor [6] has proposed a physical model of the tokamak interior which leads to reasonable predictions of its natural profiles, without relying on an *ad hoc* variational principle. His physical model, which owes much to the "clump" picture of MHD turbulence put forth by Tetreault [7], is instructive and serves as the basis for our study. We adopt Taylor's model of the tokamak interior, which is characterized by filamented currents running along stochastic magnetic field lines. In this model, the current filaments interact collectively to determine the overall magnetic field in a steady state. We study the effect of the plasma internal current, via this interaction, on the magnetic surfaces imposed on the plasma through a given field.

II. Tokamak Interior Model

In a slow-moving or equilibrium plasma in a tokamak, we consider the combined internal and external toroidal and poloidal magnetic fields to take the form

$$\mathbf{B} = B_0(\hat{\mathbf{z}} + \hat{\mathbf{z}} \times \nabla\Psi) \ , \tag{1}$$

where the poloidal field is related to the toroidal current by

$$\mathbf{J} = J\hat{\mathbf{z}} = \boldsymbol{\nabla} \times \mathbf{B} = (\nabla^2\Psi)\hat{\mathbf{z}} \ . \tag{2}$$

Here, the current and magnetic field satisfy

$$\boldsymbol{\nabla} \times (\mathbf{J} \times \mathbf{B}) = 0 \ . \tag{3}$$

Were the magnetic field regular and endowed with perfect surfaces, such that $\mathbf{B} \cdot \nabla\Psi = 0$, then (3) would be satisfied automatically and (2) alone would determine the current profiles, though with a great degree of generality left unresolved. We suppose instead that the magnetic field is weakly ergodic: it does not possess perfect surfaces, nor does it wander uniformly throughout the toroidal volume. Small turbulent effects cause the field line to vary from the ideal surfaces only slowly. A line must traverse many circuits of the torus to deviate significantly from a surface. This causes it to lose memory of its past and breaks the strict periodicity of the torus. Since a field line that wanders through a constantly changing torus is equivalent to one wandering through an infinite cylinder, we treat our volume as such a cylinder.

A non-uniformly distributed current flows along the magnetic field lines which become stochastic when magnetic islands begin to overlap. Neighboring field lines will carry their currents alongside each other for roughly a Lyapunov time, after which the field lines diffuse apart. At the same time, however, new current filaments are brought together by the action of the stochastic field lines.

Equation (3) can be written as

$$\frac{\partial J}{\partial z} + [\Psi, J] = 0 \ , \tag{4}$$

where $[\ldots]$ indicates the usual Poisson bracket in the poloidal coordinates. From (4) it is plain that with z acting as a time-like variable, Ψ acts as a Hamiltonian describing the evolution of the toroidal current. We represent the current as a collection of filaments of strength κ_i:

$$J(\mathbf{r}, z) = \sum_i \kappa_i \delta(\mathbf{r} - \mathbf{r}_i(z)) \ . \tag{5}$$

The filaments' positions evolve according the Hamiltonian equations

$$\kappa_i \frac{d\mathbf{r}_i}{dz} = \hat{\mathbf{z}} \times \frac{\partial H(\mathbf{r}_1, \ldots, \mathbf{r}_N; z)}{\partial \mathbf{r}_i} \ , \tag{6}$$

where $\sqrt{\kappa_i}\, x_i$ is conjugate to $\sqrt{\kappa_i}\, y_i$, and the part of the Hamiltonian is played by the flux function Ψ.

This discretization may be looked upon as a representation of the nature of flux found in a real tokamak, but may more generally be considered as a mathematical procedure in which the number of degrees of freedom representing the current field is reduced from the continuum infinity of a field variable to the discrete infinity of a set of filament positions, which may even be represented by a large but finite number of filaments in order to be handled computationally. A complete description of this procedure is given in Ref. [8].

The essential point is the realization that because our system is governed by a Hamiltonian set of equations, conventional statistical mechanics can be used to find reasonable (and physically justifiable) current profiles. The randomization necessary to perform statistical mechanics comes not from strong turbulence in the fluid, which would not be compatible with typical tokamak operations, but from the stochasticity of the magnetic field. Assuming all filaments have equal strength κ, one may define a statistical distribution function of filament positions $\rho(\mathbf{r}_1, \ldots, \mathbf{r}_N)$, adopt a microcanonical ensemble and calculate the mean

current distribution as

$$J(\mathbf{r}) = \kappa \langle \rho(\mathbf{r}) \rangle = \text{const.} \int \delta[E - H(\mathbf{r}, \mathbf{r}_2, \ldots, \mathbf{r}_N)] \prod_2^N d\mathbf{r}_i \ . \tag{7}$$

The mean filament density can be found using information theory techniques, and leads to the result

$$J(\mathbf{r}) = K e^{-\mu\kappa\Psi(\mathbf{r})} \ , \tag{8}$$

which, together with the equilibrium equation (2), gives the profile (see [6] and [8])

$$J = \frac{J_0}{\left(1 + \alpha \frac{r^2}{a^2}\right)^2} \ . \tag{9}$$

III. Interior Model with External Applied Field

Our purpose now, however, is not to determine natural current profiles in a tokamak, but rather to make use of this interacting field-line model to explore the structure of magnetic surfaces inside a tokamak. We treat the profile of Eq. (9) as a given externally-imposed helical magnetic field. Local deviations from the background current are treated as small current filaments running along the background magnetic field lines. The structure of the total field is determined by the action of these interacting filaments on top of the basic structure of the imposed field. Thus we assume the following form for the flux-function Hamiltonian:

$$H \equiv \Psi = \sum_i \kappa_i [\Psi_{\text{ext}}(\mathbf{r}_i) + \Psi_{\text{int}}(\mathbf{r}_i)] \ , \tag{10}$$

where we write

$$\Psi_{\text{int}}(\mathbf{r}_i) = \sum_{j<i} \frac{\kappa_j}{4\pi} \ln |\mathbf{r}_i - \mathbf{r}_j| \ , \tag{11}$$

the appropriate flux for a system of parallel currents in two dimensions. Ψ_{int} represents the mutual interaction of the current-carrying filaments. The first term of (10) is the external field, which we take to be confined to a particular helical mode and hence to be of the

following form:

$$\Psi_{\rm ext}(\mathbf{r}) = \Psi_0(\mathbf{r}) + \sum_{m,n} U_{mn} e^{i(m\theta - n\phi)} \ , \tag{12}$$

where $\phi = z/R$, and the U's are assumed to depend only weakly on $\mathbf{r}$. As an approximation, we write

$$U_{mn} = \begin{cases} \frac{1}{2}U = \text{constant} & m = \pm m_0, n = \ell n_0 \quad (\ell \text{ an integer}) \ . \\ 0 & \text{otherwise} \ . \end{cases} \tag{13}$$

We expand Ψ_0 to second order around r_0 (where $q(r_0) = m_0/n_0$). The toroidal coordinate z plays the role of time, and hereafter, we will write t in place of z.

Under the assumption of (13), (6) and (12) lead to the equations of motion for the current filaments (see Appendix):

$$\begin{aligned} \frac{dx_i}{dt} &= U \sin(2\pi y_i) \sum_n \delta(t-n) - \sum_{j\neq i} \frac{\kappa_j}{2\pi} \frac{\sigma^2 (y_i - y_j)}{(x_i - x_j)^2 + (y_i - y_j)^2} \ , \\ \frac{dy_i}{dt} &= x_i + \sum_{j\neq i} \frac{\kappa_j}{2\pi} \frac{x_i - x_j}{(x_i - x_j)^2 + (y_i - y_j)^2} \ , \end{aligned} \tag{14}$$

with

$x = \frac{\sigma m_0}{2\pi r_0}(r - r_0)$ a rescaled radial coordinate,

$y = \frac{(m_0\theta - n_0\phi)}{2\pi}$ a helical angular coordinate,

$t = \frac{n_0 z}{R}$ the time-like toroidal coordinate,

and

$\sigma = \frac{2\pi}{m_0} \frac{d\ln|\frac{1}{q}|}{d\ln r}\Big|_{r_0}$ proportional to the magnetic shear.

The interaction of the background current filaments is represented by the first terms in the right-hand side of Eq. (14), while random local deviations from this current are represented by the parameters κ_i's which take on individual values centred around 0 and whose interaction is represented by the second terms in the right-hand side of (14).

IV. The Standard Map

The portion of the filament motion due to the externally applied current in (14) (that is, the first terms of the right-hand side) can be represented by the "standard map," a well-known non-linear map which has been studied both for its own interest and as a model for various physical systems (See, e.g. [9] and [10]). The toroidal projection of our unperturbed magnetic field lines is given by successive iterations of this map, defined by:

$$\begin{aligned} y_{n+1} &= y_n + x_n \\ x_{n+1} &= x_n + U \sin(2\pi y_{n+1}) \ . \end{aligned} \tag{15}$$

The map is characterized by stable orbits surrounded by stochastic regions, the areas of which increase with the parameter U. For a critical value of U near 0.1546, the stochastic regions of adjacent orbits overlap, and trajectories diffuse throughout the region without limit. For $U < U_{\text{crit}}$ trajectories stay confined within one particular orbit. Thus, a weak external field will produce magnetic surfaces that are distinct and separate, with individual field lines confined to roughly concentric tori. Under a stronger applied field, surfaces will overlap and the volume will approach one large stochastic region, with a single field line wandering ergodically throughout the region. Figure 1 shows stochastic regions for $U < U_{\text{crit}}$ and $U > U_{\text{crit}}$.

Another feature of the standard map are the "accelerator modes" [10]. These modes are present only for particular values of $U \gg U_{\text{crit}}$ such that when U takes on one of these (near-integral) values, there exist particular regions of phase space in which a trajectory may become greatly accelerated in x. The displacement of trajectories in this region grows faster than linearly with time (whereas over most of the phase space, diffusion is linear), although they eventually diffuse out of the accelerating region altogether, to diffuse at the normal rate.

V. Computational model

The interaction term of (14) also takes a well-known form. Hydrodynamical vortices [11] and two-dimensional guiding-centre plasmas [12] (in which particles move exclusively under the $\mathbf{E} \times \mathbf{B}$ force) both have equations of motion identical to ours, apart from scaling factors. We simulate this system with a 2-d electrostatic particle-in-cell technique. The code accumulates the filament density onto a grid from the filament positions. From this filament density, it calculates the electric potential $\Psi_{\rm int}$ and field in Fourier space via Poisson's equation, Eq. (2). The field is then interpolated back to the filaments' positions to advance them forward in time. Calculations are performed for 1024 filaments on a 32×32 grid with periodic boundary conditions. On top of the interaction motion, we impose the action of the standard map. We let these "kicks" from the external field occur every 25 time steps. With the filament interaction strengths set to zero, we have measured the variance of diffusion times with U and obtained agreement with Chirikov's calculations [9]. These are shown in Fig. 2.

The computational grid represents the phase-space region $0 < y < 1$, $-1 < x < 1$, with a magnetic shear value $\sigma = 2$ in Eq. (14). Filaments are given random strengths between $+\kappa$ and $-\kappa$ with mean zero, and were initially distributed randomly throughout $0 < y < 1$, $-1/2 < x < 1/2$. We calculate the diffusion time by fitting the curve

$$\frac{1}{N} \sum_i |x_i(t) - x_i(0)|^2 = \frac{t}{T_{\rm diff}} \,. \tag{16}$$

For particularly slow diffusion, $T_{\rm diff}$ was measured by calculating the average time elapsed for a filament to first drift one unit in x from its starting position.

VI. Results

We are interested in the "time" scale of filament "diffusion." This determines the degree to which the ideal magnetic surfaces from the external current are maintained under the effects

of internal current self-interaction in a tokamak equilibrium. It is important to remember that what we measure is not actually a diffusion time: our "time" is really the toroidal coordinate ϕ. Hence the "diffusion time" is the number of revolutions around the torus that a field line must traverse in order to deviate significantly from its original surface.

The diffusion of field lines is characterized by three regimes. When U is large, the stochasticity of the standard map dominates the diffusion. As $U \to U_{\text{crit}}$, the background magnetic surfaces become regular and the diffusion is driven by the current interaction. In between is a regime wherein the diffusion rates of the two effects are comparable. Figure 3 show plots of the diffusion vs. time in the three regimes. In the field-dominated regime, the magnetic surfaces overlap, so the filaments wander throughout the region more or less freely. When the rates become comparable, a filament will spend a long time within a particular orbit before diffusing across a boundary, so the diffusion fluctuates around a mean linear growth. Finally, as $U \to 0$, the closed orbits narrow, and the fluctuations decrease in magnitude until the diffusion becomes smooth in the current-dominated regime. Figure 4 shows the dependence of diffusion time on U for different fixed values of the interaction κ. From this, one can see that the transition between the three regimes is smooth: the fluctuations around the mean diffusion appear and disappear without affecting the net diffusion rate.

Figure 5 shows the dependence of diffusion time on κ. In the absence of a background field, the current-dominated diffusion goes as $\sim \kappa^{-2}$. As κ grows large, the diffusion conforms to this law regardless of U. A qualitative look at this figure reveals that this regime sets in at around $\ln|\kappa| \approx -4.5$. When $U > U_{\text{crit}}$ the curve will flatten out as $\kappa \to 0$ (*'s in figure), making diffusion independent of κ and representing the field-dominated regime. Note that this regime does not exist for $U < U_{\text{crit}}$, as the diffusion time will increase without bound as $\kappa \to 0$, the rate of this increase growing inversely with U.

One possible anticipated effect of filament interaction was that a filament would be jostled out of an orbit's stochastic region and into a more tightly bound region, thus possibly slowing

the diffusive process. This was indicated in some simulations involving only two filaments [13] but in none of our simulations was this observed. Without exception, diffusion of magnetic surfaces was enhanced by filament self-interaction. This effect may yet be observed with a smaller number of filaments in the system, but we expect that for a realistic model of a tokamak interior, a large number of filaments must be maintained, and the anticipated diffusion inhibition would not appear in experiments.

The presence of accelerator modes of the standard map continued to be observable for small values of κ. Figure 6 shows the presence of accelerator modes in our model. They are represented by dips in the diffusion time at $U \approx 1.1$, 2.2, and 3.2, where the presence of these modes increases the general rate of diffusion. The effects of these modes can be seen for values of κ up to about the order of U_{crit}, after which the effect becomes indiscernible.

VII. Discussion

We find the effect of the interaction of local current deviations to be pronounced. When the interaction reaches a strength $\kappa \sim U_{\text{crit}}$, the accelerator modes cease to become noticeable. The parameter regime for which the field is stochastic ranges over all values of U, whereas for the unperturbed case, the field is stochastic only for $U > U_{\text{crit}}$. In the "field-dominated" regime, the stochasticity is due to the normal overlapping of magnetic islands, but even as the magnetic surfaces become regular, the plasma becomes "current-dominated" and the field remains stochastic due to filament interactions. The onset of this regime occurs when κ is near $0.011U$ when U is near the critical value of 0.155.

In addition to the questions treated herein, this model may also be applicable to the problem of the "ergodic limiter" [14], in which the role of the limiter in a tokamak is played by stochastic field lines. The filamentary features of currents and magnetic fields are well-noted of late in astrophysical plasmas as well [15, 16]. Similon and Sudan [17] studied the Alfvén wave propagation in the stochastic fields of solar coronal loops in which a toroidal

magnetic field is present. The present model may be relevant to such astrophysical plasmas as well. Finally, current filaments and their stochastic behavior in condensed matter [18] may be treated in a similar manner.

Acknowledgments

We have appreciated discussions with Professor J.B. Taylor. This work was supported in part by U.S. Department of Energy grant DE-FG05-80ET53088, by NSF Grant ATM8811128, and by the JIFT program, under which one of the authors (H.I.) was visiting the IFS during the completion of part of this work.

Appendix

Here we derive the map describing the dynamics of the field line due to the applied external current. The field line is described by

$$\frac{dr}{d\phi} = \frac{B_r}{B_0} , \quad \frac{d\theta}{d\phi} = \frac{B_\theta}{rB_0} \phi = \frac{z}{R} . \tag{A1}$$

Define

$$\Phi = \frac{\Psi}{L} , \qquad I = \frac{r^2}{2LR} , \tag{A2}$$

as normalized poloidal and toroidal flux. L is an arbitrary quantity with dimensions of length. The coordinates I and θ obey the Hamiltonian equations with ϕ as the time coordinate:

$$\frac{dI}{d\phi} = \frac{\partial\Phi}{\partial\theta}\frac{d\theta}{d\phi} = \frac{\partial\Phi}{\partial I} . \tag{A3}$$

Let us change coordinates from (I, θ) to (ρ, η) by way of a canonical transformation with the generating function

$$F(\rho, \theta; \phi) = \rho(m_0\theta - n_0\phi) + I_0\theta . \tag{A4}$$

Our new coordinates are determined by the equations

$$\begin{aligned} I &= \frac{\partial F}{\partial\theta} = m_0\rho + I_0 \\ \eta &= \frac{\partial\Phi}{\rho} = m_0\theta - n_0\phi , \end{aligned} \tag{A5}$$

while the "Hamiltonian" transforms like

$$\Phi_{\text{new}} = \Phi_{\text{old}} + \frac{\partial\Phi}{\partial\phi} . \tag{A6}$$

We treat the case in which Φ (in (I, θ) coordinates) looks like

$$\Phi = \Phi_0(I) + \sum_{m,n} U_{mn} e^{i(m\theta - n\phi)} , \tag{A7}$$

and expand Φ_0 around $I = I_0$ to second order. In (ρ, η) coordinates, Φ looks like

$$\Phi \approx \Phi_0(I) + m_0\rho\Phi_0'(I_0) + \frac{1}{2}(m_0\rho)^2\Phi_0''(I_0) + \sum_{m,n} U_{mn}e^{i(m\theta - n\phi)} - n_0\rho \ . \tag{A8}$$

If we now choose I_0 such that

$$\Phi'(I_0) = \frac{n_0}{m_0} \ , \tag{A9}$$

in other words, look at the region where the local $q = m_0/n_0$, then

$$\Phi \approx \Phi_0(I_0) + \frac{1}{2}(m_0\rho)^2\Phi_0''(I_0) + \sum_{m,n} U_{mn}e^{i\left(\frac{m}{m_0}\eta - \left(n - \frac{m}{m_0}n_0\right)\phi\right)} \ . \tag{A10}$$

Now let us assume that U_{mn} takes the form

$$U_{mn} = \begin{cases} \frac{1}{2}U = \text{constant} & m = \pm m_0, n = \ell n_0 (\ell \text{ an integer}) \ . \\ 0 & \text{otherwise} \ . \end{cases} \tag{A11}$$

This will be a valid assumption if U has a weak radial dependence or a weak q (safety factor) dependence. The summation may be rewritten in this case as

$$\frac{1}{2}U\sum_\ell e^{i(\eta - (\ell-1)n_0\phi)} + \frac{1}{2}U\sum_\ell e^{i(\eta-(\ell+1)n_0\phi)} = U\sum_\ell \cos(\eta - \ell n_0\phi) = U\cos\eta\sum_n \delta\left(\frac{n_0\phi}{2\pi} - n\right) \ . \tag{A12}$$

Our equations of motion are now

$$\begin{aligned} \tfrac{d\eta}{d\phi} &= \tfrac{\partial\Phi_{\text{new}}}{\partial p} = \Phi_0''(I_0)m_0^2 p \\ \tfrac{dp}{d\phi} &= -\tfrac{\partial\Phi_{\text{new}}}{\partial\eta} = U\sin\eta\textstyle\sum_n \delta\left(\frac{n_0\phi}{2\pi} - n\right) \ , \end{aligned} \tag{A13}$$

which give us the listed equations of motion in the transformed coordinates with the scale change

$$U \to 2\pi\Phi_0''(I_0)\left(\frac{m_0}{n_0}\right)^2 U \ . \tag{A14}$$

References

[1] J.B. Taylor, Rev. Mod. Phys. **58**, 741 (1986).

[2] V.A. Gordin and V.I. Petviashvili, Zh. Ekxp. Teor. Fiz., **95**, 1711 (1989) [Sov. Phys. JETP **68**, 988 (1989)].

A.D. Beklemishev, V.A. Gordin, R.R. Khayrutdinov, V.I. Petviasyhvili, and T. Tajima, submitted to Nucl. Fusion (1991).

[3] D. Biskamp, Comments Plasma Phys. **10**, 165 (1986).

[4] J.Y. Hsu and M.S. Chu, Phys. Fluids **30**, 1221 (1987).

[5] B.B. Kadomtsev, Sov. J. Plasma Phys. **13**, 443 (1987).

[6] J.B. Taylor, IFS preprint # 447 (1991).

[7] D.J. Tetreault, Phys. Fluilds **32**, 2122 (1988); Phys. Fluids **B1**, 511 (1989); Phys. Fluids **B2** 53 (1990).

[8] D. Montgomery, L. Turner, and G. Vahala, J. Plasma Phys. **21**, 239 (1979).

[9] B.V. Chirikov, Phys. Rep. **52**, 263 (1979).

[10] Y.H. Ichikawa, T. Kamimura, and T. Hatori in *Statistical Physics and Chaos in Fusion Plasmas*, Ed. C.W. Horton & L.E. Reichl, (John Wiley & Sons, 1984) 21.

[11] J.P. Christiansen, J. Comp. Phys. **13**, 363 (1973).

[12] W.W. Lee and H. Okuda, J. Comp. Phys. **26**, 139 (1978).

[13] Irie, private communication.

[14] W. Feneberg and G.H. Wolf, Nucl. Fusion **21**, 669 (1981).
S.C. McCool *et al.*, Nucl. Fusion **29**, 547 (1989).

[15] J.O. Stenflo, Astron. Astrophys. Rev. **1**, 3 (1989).

[16] C.T. Russell, E.R. Priest, and L.C. Lee, "Physics of Magnetic Flux Ropes" (AGU, Washington D.C., 1990).

[17] P.L. Similon and R.N. Sudan, Ap. J. **336**, 442 (1989).

[18] D.R. Nelson, Phys. Rev. Lett. **60**, 1971 (1988).

Figure Captions

1. Phase-space plot $(x_n,\ y_n)$ for 25,000 iterations of the standard map beginning at a point near the X-point, (0,0). Plot shows stochastic region of the standard map for (a) $U = 0.15 < U_{\text{crit}}$ and (b) $U = 0.20 > U_{\text{crit}}$.

2. Crosses show computed diffusion time, T_{diff}, versus the parameter U for the standard map. The solid line is the fit calculated by Chirikov [9].

3. Plots of mean square diffusion, $\frac{1}{N}\sum_i |x_i(t) - x_i(0)|^2$, vs. time for $\kappa = 10^{-4}$. (a) field-dominated regime $U = 2.0$. (b) transition regime $U = 0.15$, (c) current-dominated regime $U = 0$.

4. T_{diff}, vs. U for $\kappa = 0.05,\ 0.01,\ 10^{-3},\ 10^{-4}$, and 10^{-5}.

5. Log-log plot of T_{diff} vs. κ. The solid line represents the data from $U = 0$. The o's are from $U = 0.06$, the +'s from $U = 0.15$, and the *'s from $U = 0.20$.

6. T_{diff} vs. U in the accelerator mode regime. (a) in the absense of self-interaction, $\kappa = 0.0$. (b) for $\kappa = 0.1$. The effect is dimished but still noticeable. (c) for $\kappa = 0.2$ the modes are all but gone.

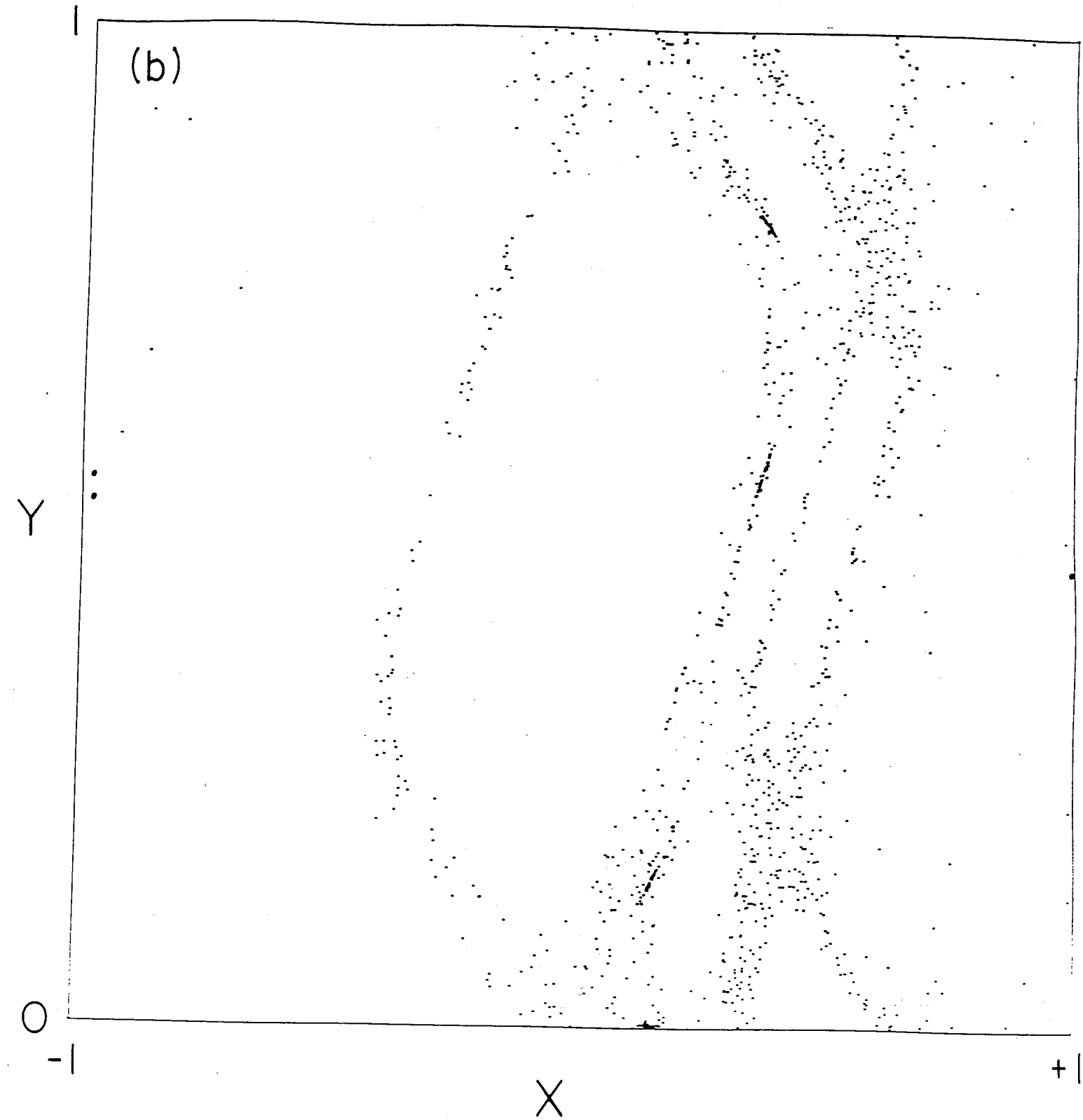

Fig. 1(a)

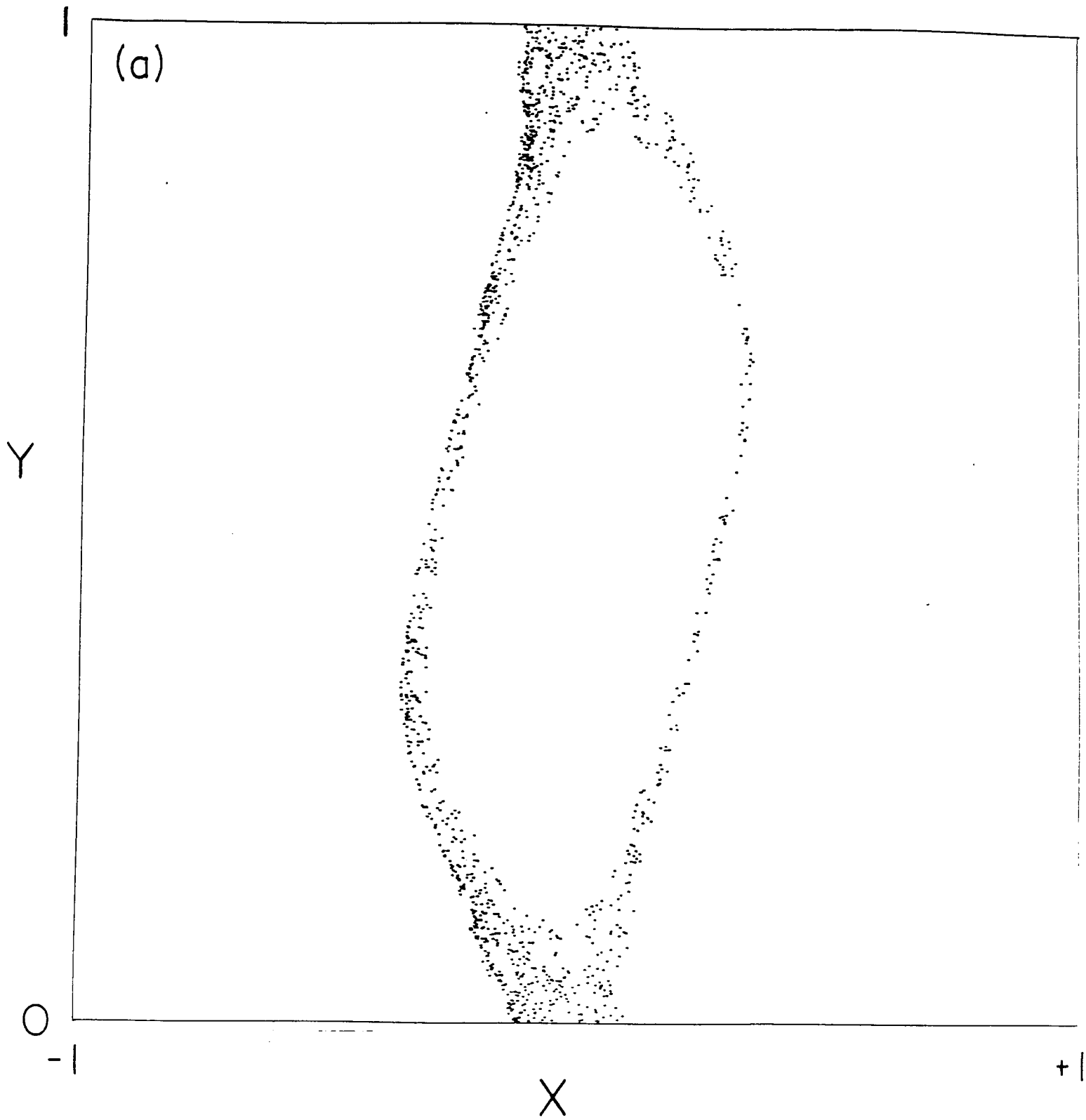

Fig. 1(b)

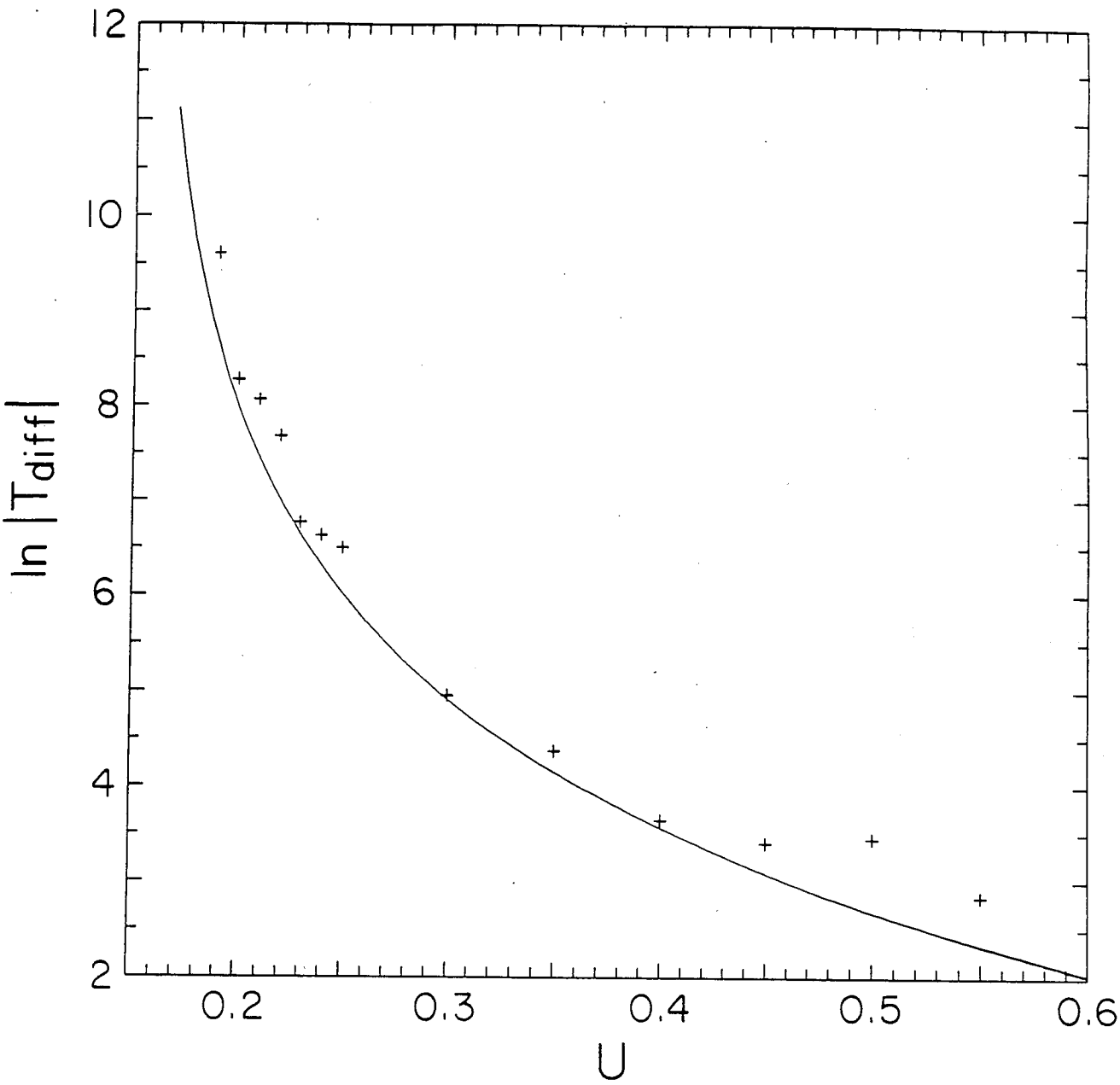

Fig. 2

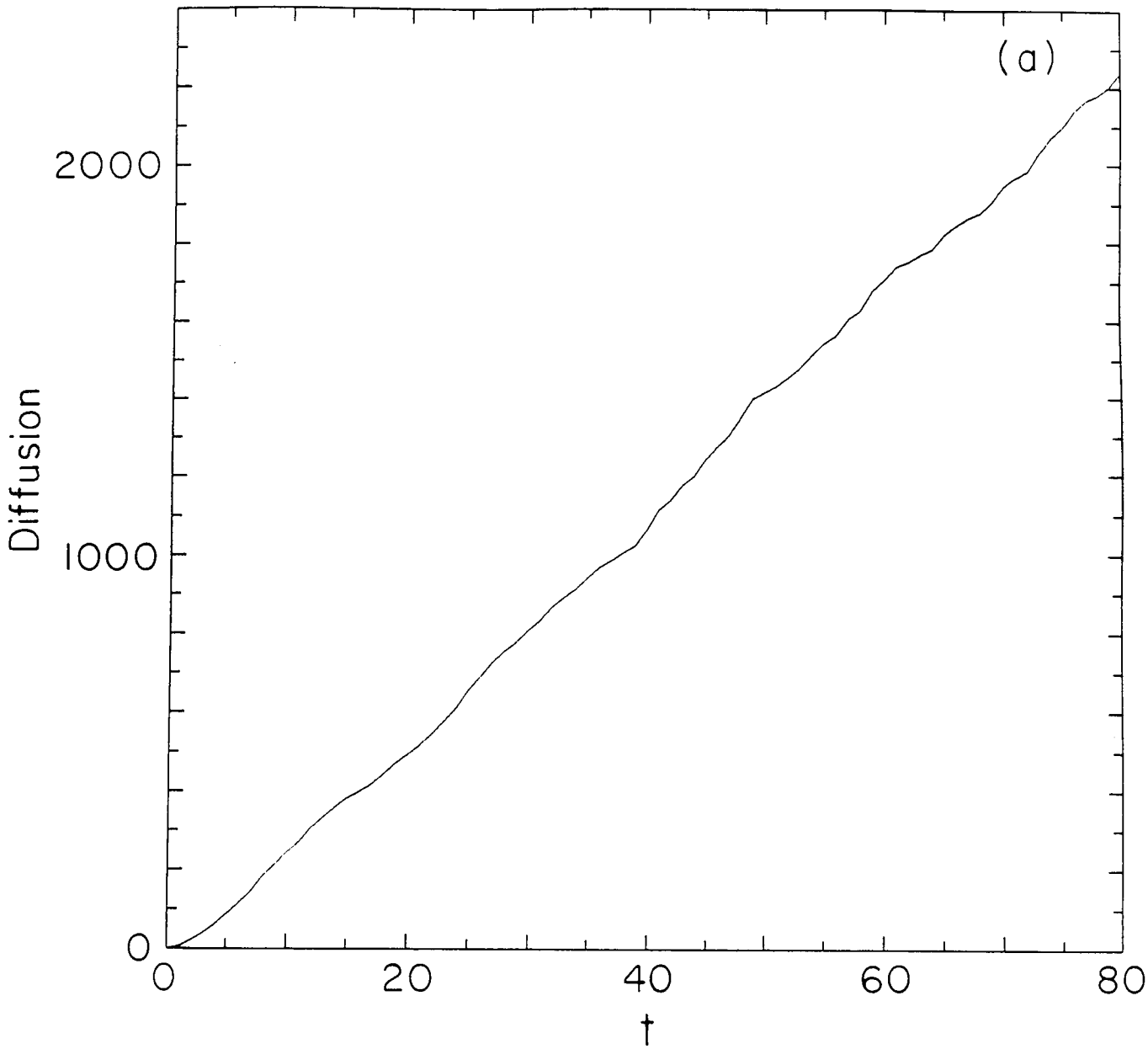

Fig. 3(a)

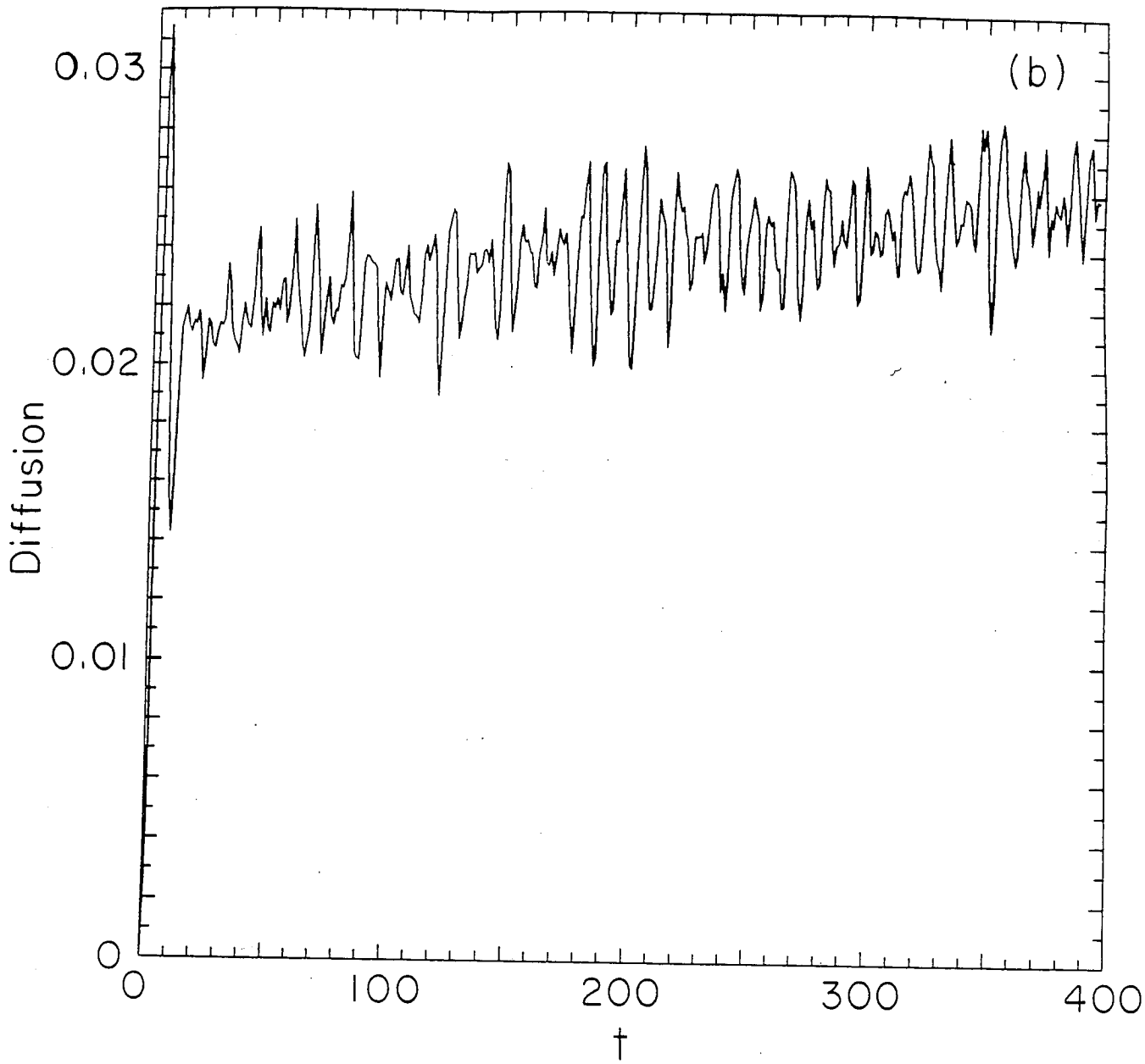

Fig. 3(b)

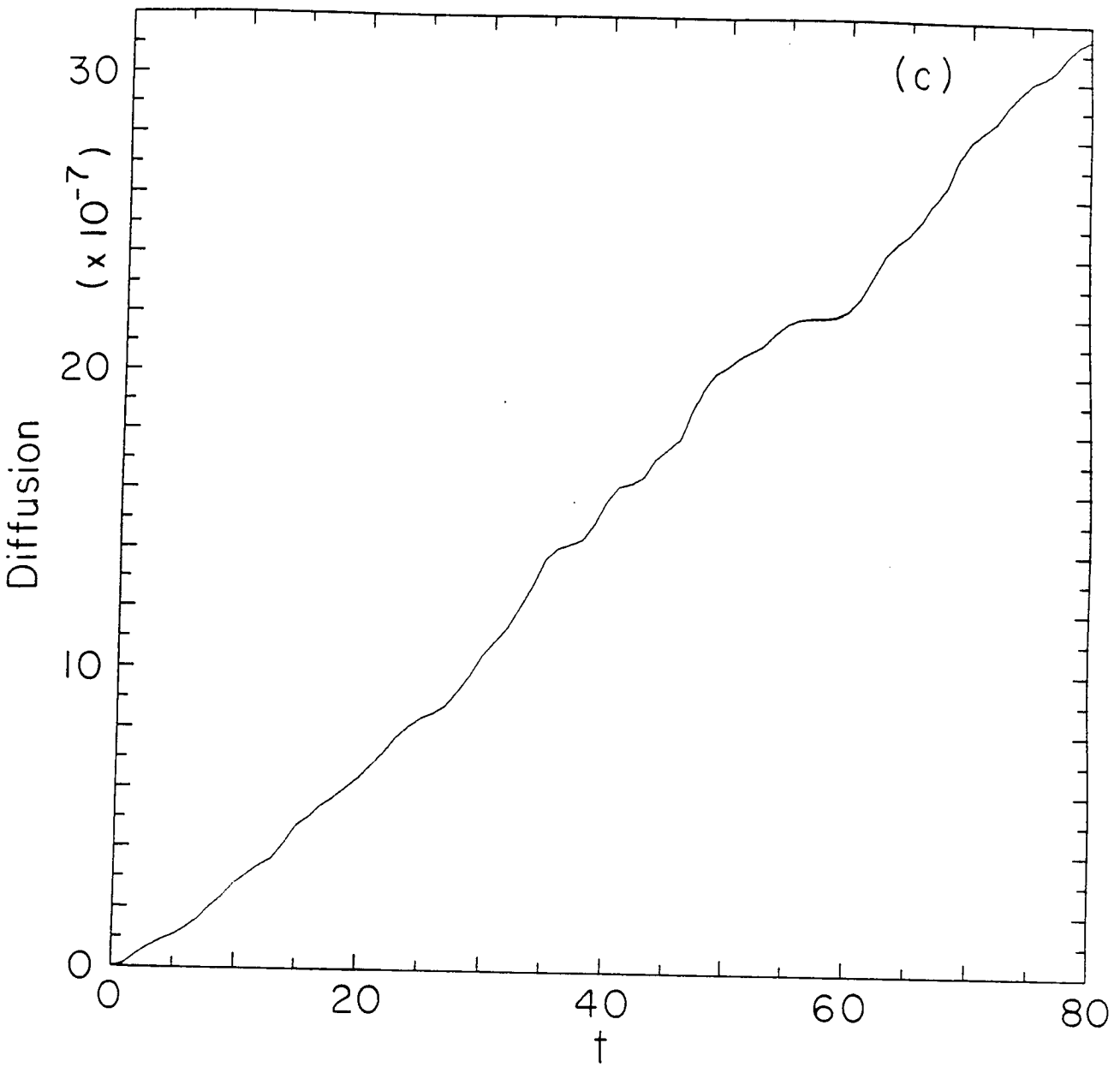

Fig. 3(c)

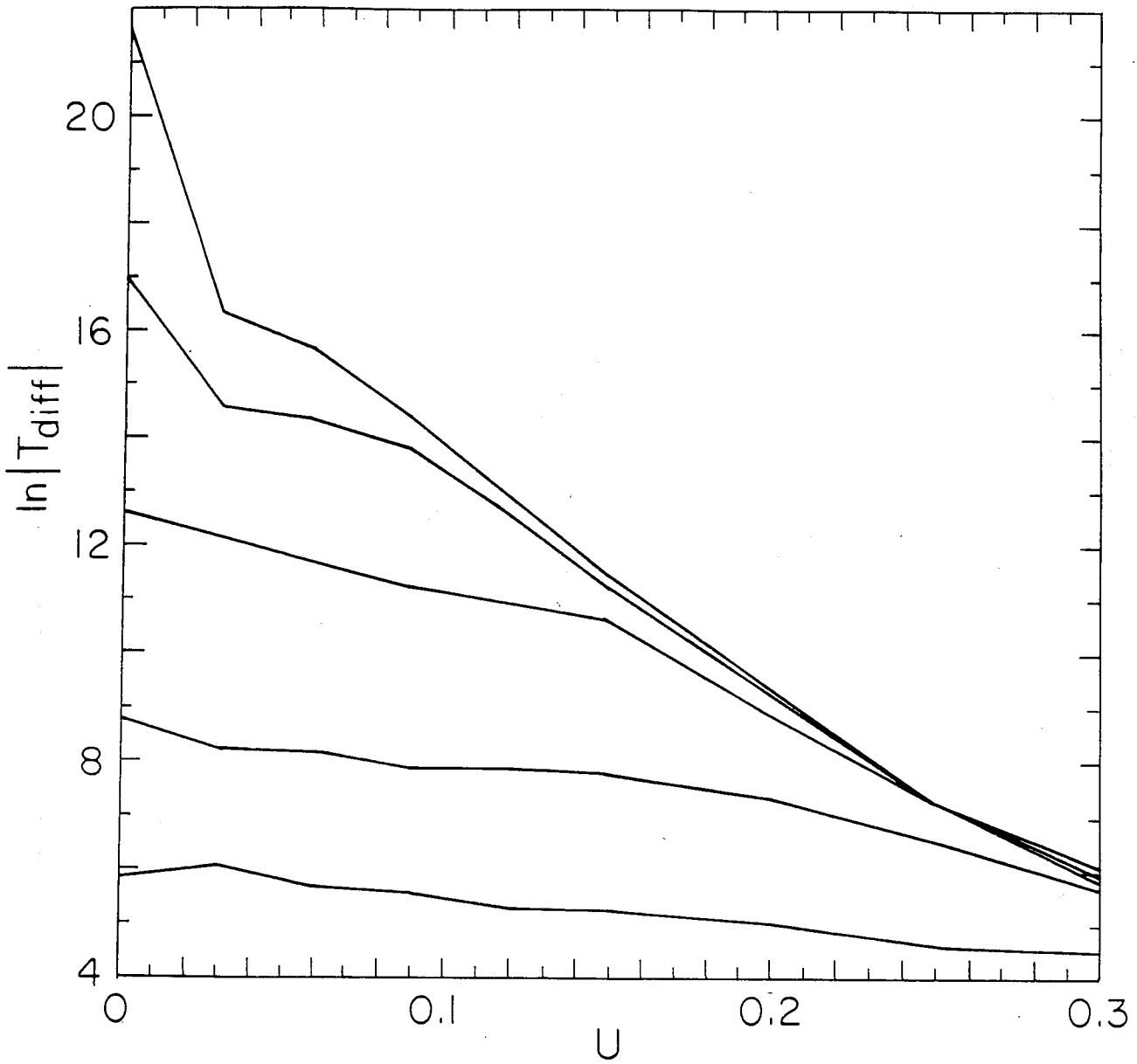

Fig. 4

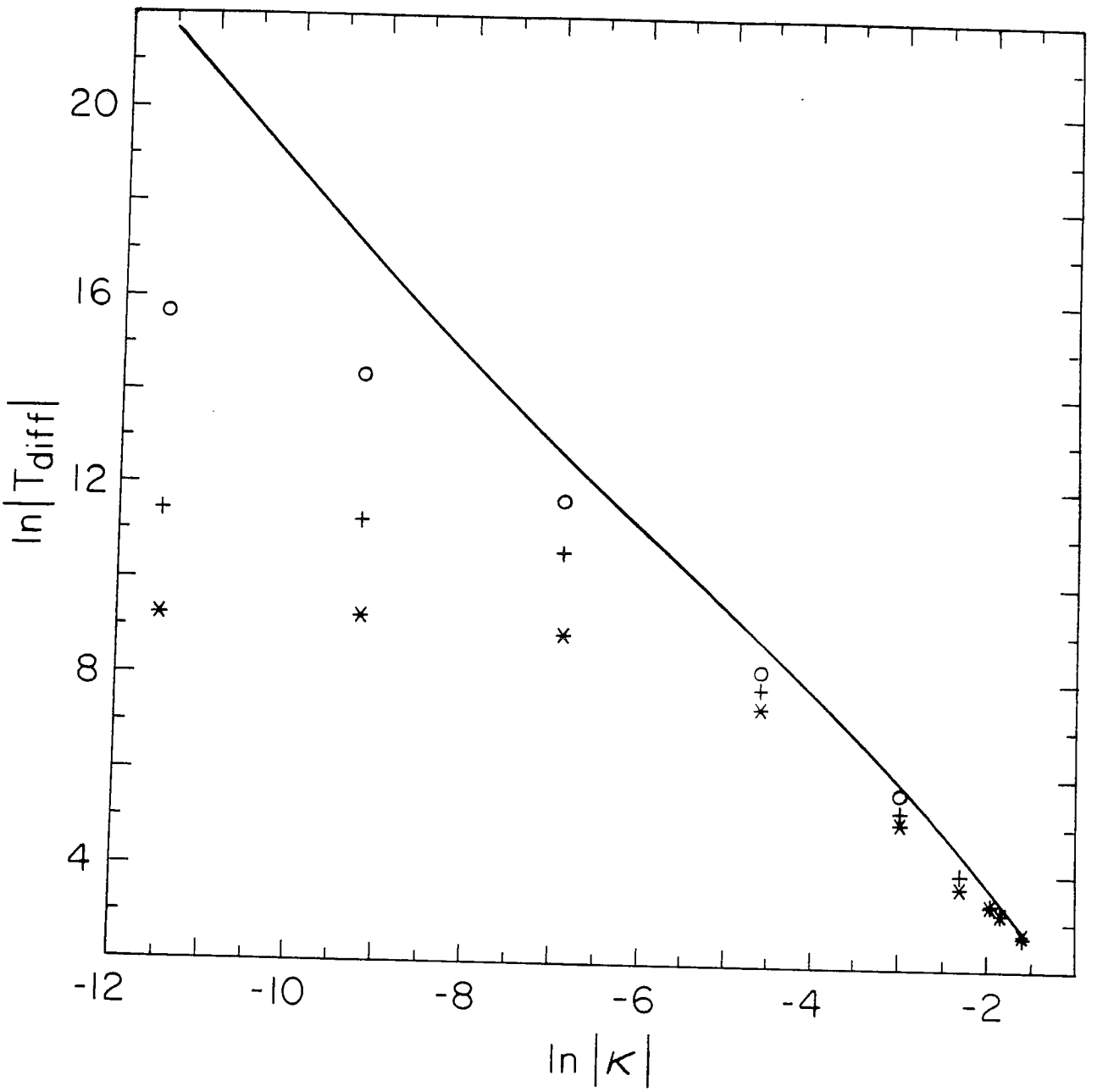

Fig. 5

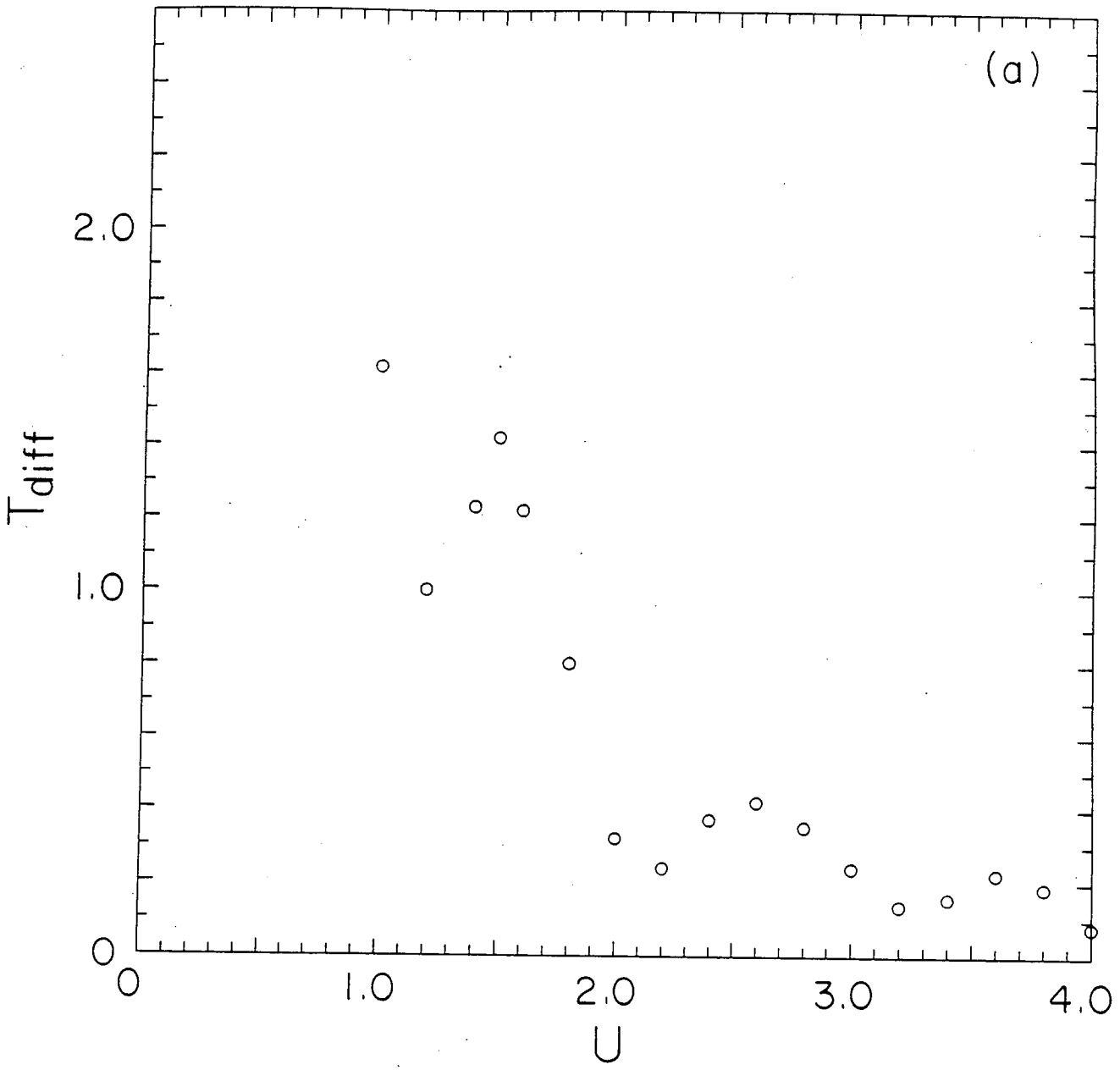

Fig. 6(a)

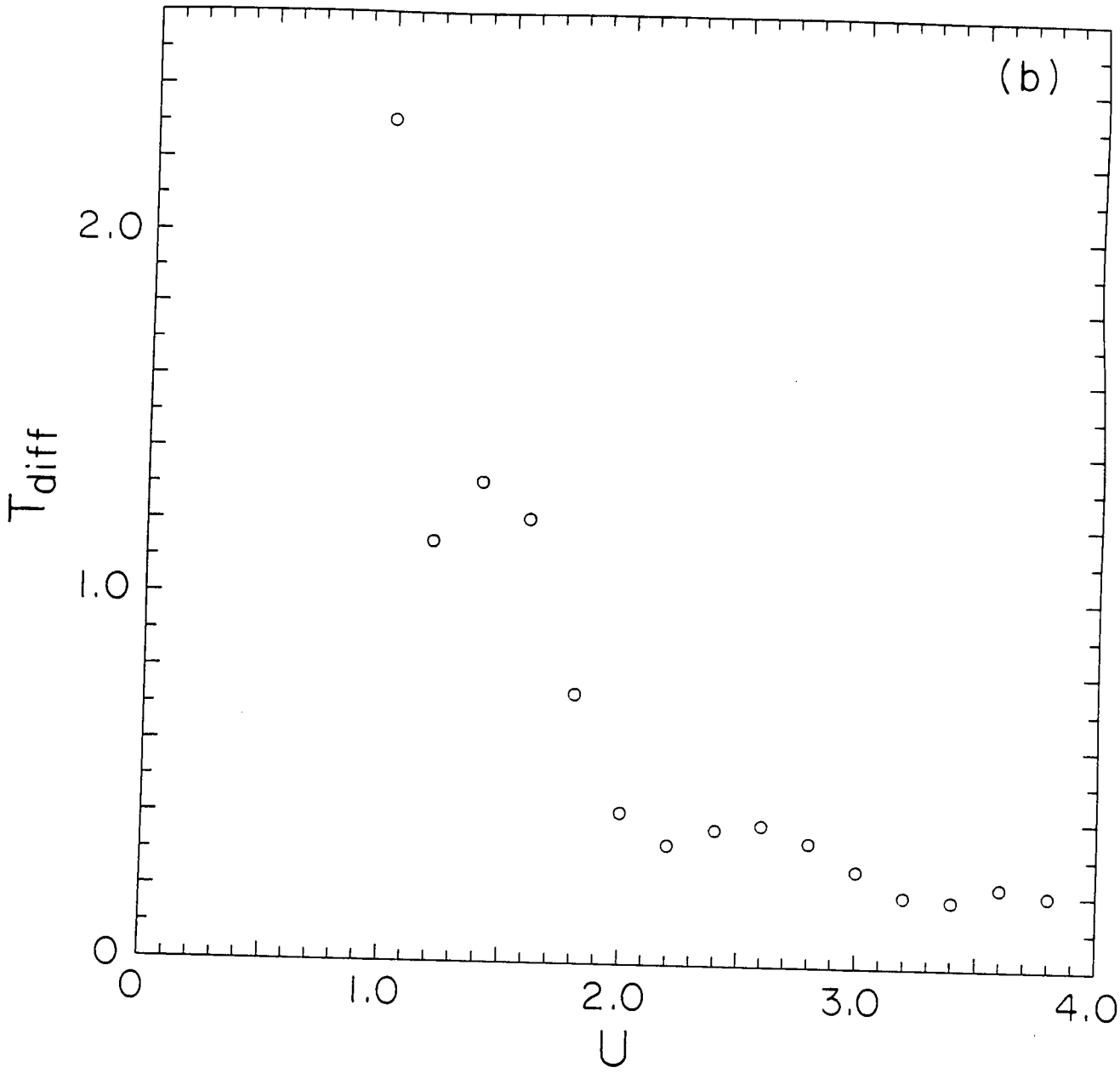

Fig. 6(b)

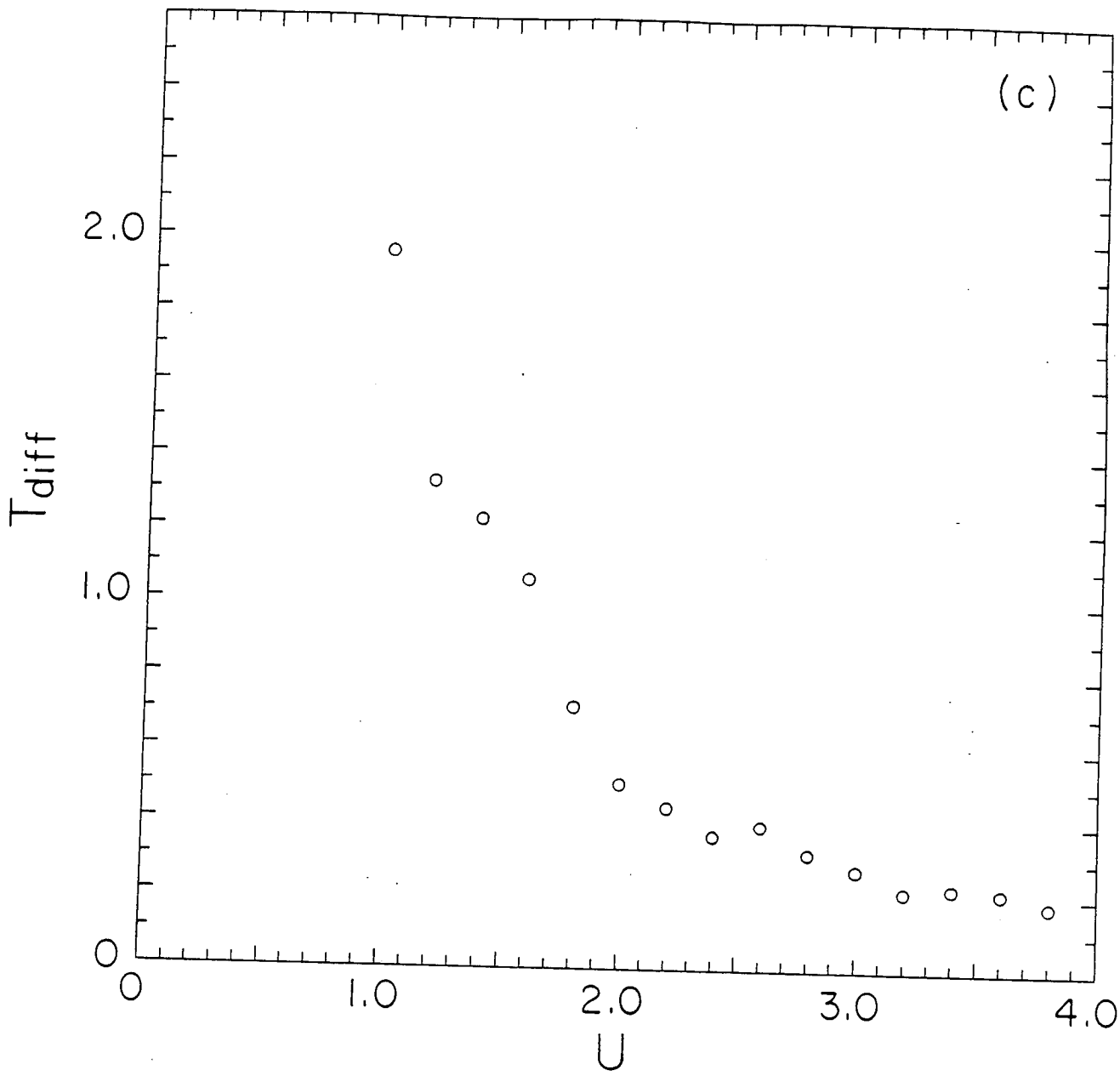

Fig. 6(c)